Photodetector properties of CdSe thin films grown by close space sublimation method

M. Ali Olgar[1,*] , Bülent M. Başol[2], İsmail Polat[3], Murat Tomakin[4], Tayfur Küçükömeroğlu[5], and Emin Bacaksız[5,*]

[1] Department of Physics, Niğde Ömer Halisdemir University, Niğde, Turkey

[2] Active Layer Parametrics, Scotts Valley, CA, USA

[3] Department of Energy Systems Engineering, Faculty of Technology, Karadeniz Technical University, Trabzon, Turkey

[4] Department of Physics, Recep Tayyip Erdoğan University, Rize, Turkey

[5] Department of Physics, Karadeniz Technical University, Trabzon, Turkey

ABSTRACT

In the present study, CdSe thin films were grown by Close Space Sublimation (CSS) method on glass substrates at elevated temperatures. The prepared films were analyzed through several characterization techniques such as XRD, SEM, EDX, optical transmission, and photoluminescence. Films had single phase hexagonal crystal structure without any obvious secondary phase segregation. The preferred orientation was (002). SEM images taken from the surface and cross-section of the layers showed well-defined faceted microstructure with a grain size ranging from 0.5 to 1.0 μm. The chemical composition was stoichiometric. Optical band gap calculated from the optical transmission was determined to be 1.73 eV. Room temperature PL spectra showed a single strong peak located at around 715 nm that can be attributed to free carrier-to-band or band-to-band optical transitions. The performance of photodetector devices constructed using the CSS grown CdSe films showed a wavelength dependent behavior, shorter wavelength light generating higher photocurrent. It was seen also determined that the responsiveness and detectivity values increased with decreasing value of the light wavelength. Switching properties, responsivity and detectivity of the photodetectors were studied. The maximum responsivity was observed at 714 nm. Devices yielded the highest photocurrent at a wavelength of 443 nm.

1 Introduction

The Cadmium selenide (CdSe) alloy, which belongs to the II–VI group semiconductor compounds, has many different optoelectronic applications. Growing CdSe both in different crystal structures, such as hexagonal and cubic, and in n and p type conductivity allow it to be used in a variety of different device structures [1, 2]. In recent years, CdSe compound has been used as an alternative material to the CdS window layer in solar cell applications. It is also used for forming a CdTeSe alloy interface between the CdTe and CdS layers of

---

the CdTe thin film solar cell structure, which yielded efficiency improvements [3, 4]. CdSe thin films can be produced by different methods and their properties can be modified by different strategies [5–8]. At the present time, researchers are using CdSe in photodetector applications since it has high photo-detection capacity in the visible-near IR radiation space. Photoresponse of CdSe thin film is principally due to photo generation, separation of the electron-hole pairs by an internal electric field, and eventual electron-hole pair recombination. Therefore, photodetector properties of CdSe thin films can be improved by either doping with an appropriate dopant or growing the films in nanostructures, where grain boundary effects are minimized [9, 10]. Alagarasan et al. obtained nanostructured CdSe thin films using a thermal evaporation system and investigated the effects of annealing temperature on the photodetector properties. They found that an annealing treatment step at 300 °C yielded the most promising photodetector parameters such as photo-responsivity and photo-detectivity [11]. Shelke et al. formed CdSe thin films by spray pyrolysis. They obtained as-deposited CdSe films with high photoperformance, exhibiting quick response and decay times of 24 and 95 ms, respectively [12]. In an another study, CdSe thin films were produced at substrate temperatures of up to 250 °C using a thermal evaporation process. Higher responsiveness, detectivity and external quantum efficiency values were obtained in CdSe films produced at 200 °C compared to films produced at other substrate temperatures [13]. Li et al. have investigated the saturation vapor pressure and its temperature dependence, and noted that evaporation of CdSe at above 1 Pa pressure would require a temperature above 750 °C [10]. At high source temperatures CdSe decomposes into Cd and Se_2 species as seen in Eq. 1 below. At low enough substrate temperatures, highly stoichiometric, homogeneous and single phase CdSe thin films may form on the substrate as a result of the reaction of Cd and Se_2 species.

$$CdSe \longleftrightarrow Cd\,(g) + 1/2Se_2(g). \tag{1}$$
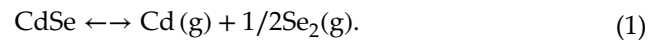
References to some other studies on photodetector applications of CdSe are summarized in Table 1 along with the present study, to demonstrate how our work differs from prior art.

Although there are many reported studies on the growth of CdTe by Close Space Sublimation (CSS) method, there has been only a limited amount of work on the CSS growth of CdSe films [10, 11]. Within these limited number of reports there has not been a study on the photoconductivity in CSS grown CdSe layers. In that respect, the present work is the first study in which the photoconductive properties of CSS grown CdSe films are reported. Close Space Sublimation is a large-scale manufacturing method that is used for fabrication of several giga-watts of CdTe solar cells and modules every year. It is a very fast and economical method. With this study we have demonstrated that this widely commercialized method can also be used to produce CdSe thin films, which can be employed for fabrication of photodetector devices.

2 Experimental

CdSe films were grown on soda lime glass sheets by the CSS method. 40 mg of CdSe powder with 99.95% purity was used as the source material. The distance between the substrate and the source was adjusted to about 2 mm. The source and substrate temperatures were fixed at 680 and 640 °C, respectively, and the CdSe powder was evaporated in an argon atmosphere at 2 Torr pressure. The schematic drawing of the CSS system used for the growth of the CdSe layers is shown in Fig. 1.

The thickness of the films was measured using a Dektak surface profilometer. To fabricate devices, Ti metal contacts were evaporated on CdSe layers using a suitable mask with an inter-contact distance

Table 1 Some previously reported studies on photodetector applications of CdSe films prepared by different methods
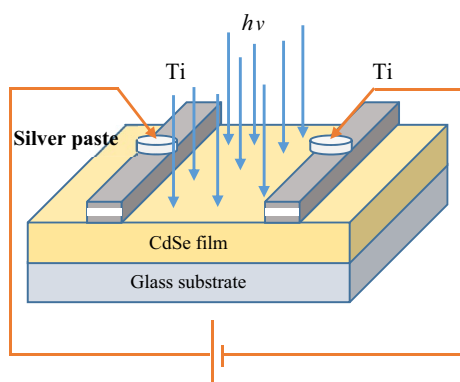
References	Substrate	Method	Sample
[14]	NaCI single crsytal	DC sputtering	2D CdSe film
[15]	Glass	Thermal evaporation	CdSe thin film
[16]	Si	DC sputtering	2D CdSe film
[17]	–	Direct vapor transport	CdSe crystal
[18]	Si/SiO$_2$	Vapor phase eposition	CdSe thin film
Present study	Glass	Close space sublimation	CdSe thin film
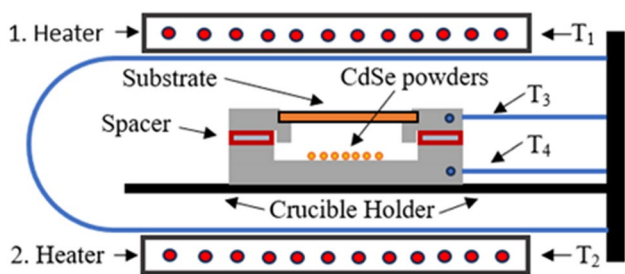
Fig. 1 Schematic diagram of the CSS system used for the growth of the CdSe thin films

of 200 μm. Contact evaporation was carried out on samples at room temperature. A schematic drawing of the device structure is shown in Fig. 2.

X-Ray diffraction (XRD) patterns were obtained using a Rigaku SmartLab Unit at measurement steps of 0.02° (between 2θ values of 5° and 70°) employing CuK$_\alpha$ ($\lambda = 1.5405$ Å) radiation. Surface morphological studies were carried out using a Scanning Electron Microscope (SEM, Zeiss) operating at an accelerating voltage of 15 kV. Elemental analysis was performed by EDAX (Energy-dispersive X-ray Analyzer) technique attached to the SEM tool. Optical transmittance spectra were measured by a Sectramax M5 spectrophotometer (using a Xe lamp with a150 W power) in the wavelength range of 500–1000 nm. Such data was taken from a few points on the sample to make sure results were repeatable. Room temperature photoluminescence data was obtained using a Dongwoo Optron spectrophotometer in the wavelength range of 600–950 nm. Light source for this measurement was a 80 mW–532 nm laser. The intensity of the light was adjusted to the same value for each wavelength during the measurement by changing the distance between

the source and the material. The resistivity and carrier concentration were measured at room temperature using Van der Pauw and Hall effect methods employing a Keithley 2410 source-meter. Photodetector performance was evaluated using a Keithley (Keithley 2410) unit and a LED light source with variable wavelength; blue ($\lambda = 443$ nm), green ($\lambda = 523$ nm), yellow ($\lambda = 588$ nm) and red ($\lambda = 625$ nm). Intensity of the light falling on the sample, as well as the distance between the source and the sample, were kept constant for all the measurements. Photodetector responsivity as a function of wavelength was measured using a monochromatic spectrometer containing xenon lamp light source calibrated with a BPW34 silicon photodiode.

3 Results and discussion

The XRD data obtained from a CdSe film grown by CSS is given in Fig. 3. As can be seen from this figure, the material grew with a (002) preferential orientation. The characteristic (102), (103), (112), (004), (203), (212) and (213) peaks of the hexagonal phase (Card No: 00-008-0459) are also present at $2\theta = 35.08$, 45.74, 49.53, 52.13, 63.83, 72.09 and 79.53°, respectively. The crystallite size of the film was calculated employing Debye-Scherrer formula utilizing (002) preferential diffraction peak. The crystallite size was found to be 38 nm. The lattice parameters were determined as $a = 0.42$ and $c = 0.70$ nm. XRD data suggests a single-phase material with no appreciable secondary phases present.

**Fig. 2** Schematic drawing of the CdSe photodetector device
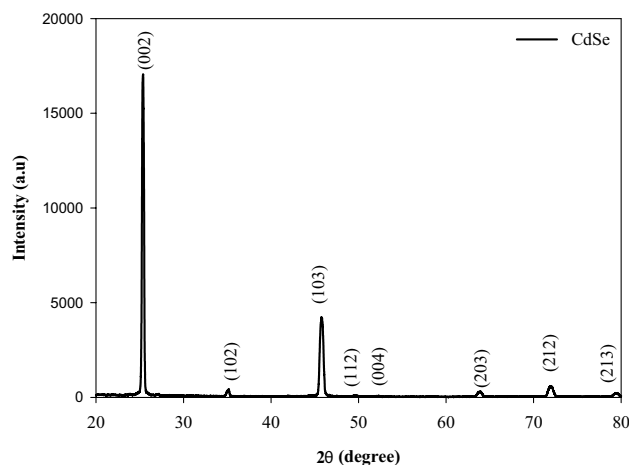
Fig. 3 XRD pattern of the CdSe thin film prepared by the CSS method

Surface and cross-sectional SEM micrographs for the film of Fig. 3 are shown in Fig. 4. As can be seen, the degree of crystallization in this material is good, grains covering the glass substrate surface well, indicating good surface wetting. Grain size is not uniform and the film comprises large and small grains with well-defined facets. While the grain size of CdSe films grown at low substrate temperatures by thermal evaporation method is generally in the range of a few nanometers, the grain size in our samples is in the 0.5–1.0 micrometer range as can be estimated from the scale-bar on the SEM images. Generally, the growth regimes of II–VI group semiconductor compounds are determined by the structure zone model [19].

Although the grain structure at the substrate interface may be small, increase in film thickness may lead to grain growth and larger grains. The thickness of the film in Fig. 4 is in the order 1.0–1.8 μm as shown in the cross-sectional view (Fig. 4b). The chemical composition was examined by EDS and the Cd/Se atomic ratio was found to be 1, indicating stoichiometric composition.

The transmittance spectra, absorption and photoluminescence data obtained are given in Fig. 5a–c. As can be seen from this data, optical transmittance increases at around 716 nm. This value approximately corresponds to the optical absorption edge for CdSe. The band gap energy value was calculated

Fig. 4 SEM micrograph of a CdSe film; **a** top view; **b** cross-sectional view
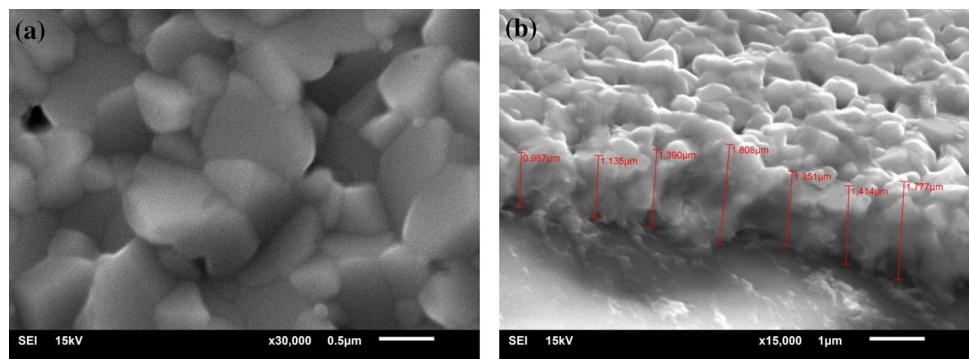
Fig. 5 The optical properties of the CdSe thin film presented by **a** transmittance, **b** $(\alpha h\nu)^2 - (h\nu)$ graph and **c** PL spectra data
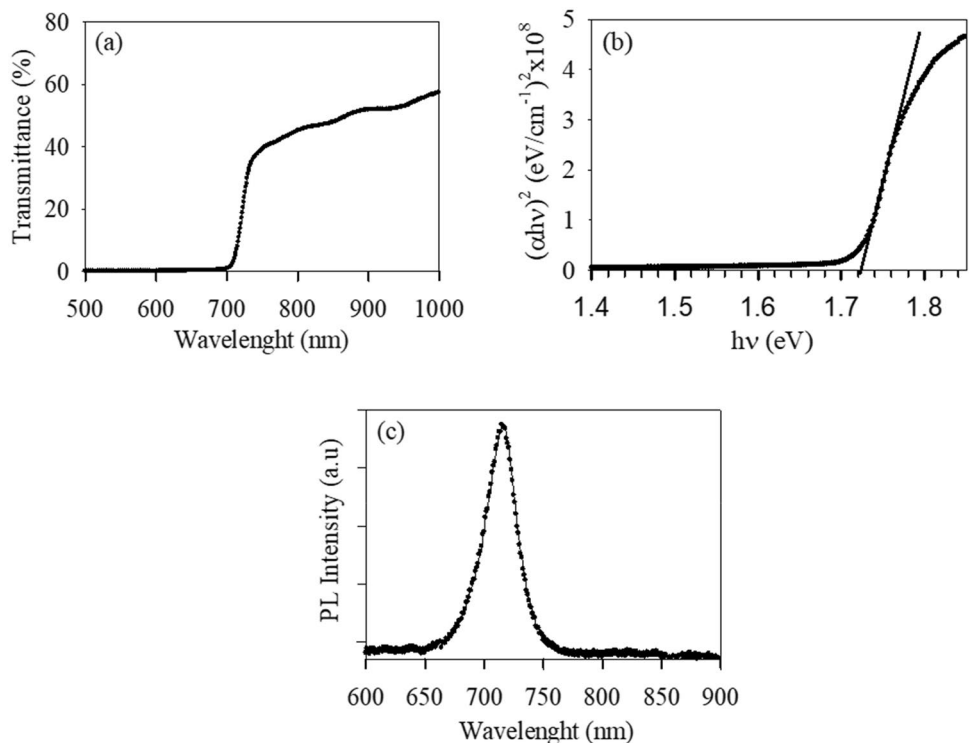
using the Tauc equation from the intercept of the extrapolated linear part of the $(ahv)^2$ curve with the energy axis. As seen in Fig. 5b, the band gap energy was found to be approximately 1.73 eV. This value matches well with the values derived for CdSe single crystals (1.72 eV) [20]. Figure 5c shows the room temperature PL spectra of the CdSe film in the UV–Visible range. As can be seen, the strong and narrow PL peak is placed at the wavelength value of 715 nm that corresponds to 1.73 eV. This is in agreement with the optical band gap value derived from Fig. 5b. Origin of the single PL peak with high intensity can be attributed to the free carrier-to-band or band-to-band optical transitions. Usually, CdSe thin films have n-type electrical conductivity since Se vacancies (V_{Se}) or Cd interstitials (Cd_i), which act as n-type centers, dominate the Cd vacancies formed during the production processes [21]. Peaks belonging to such defects were expected to show up in the high wavelength region of the PL spectrum. Absence of these peaks in Fig. 5c suggests that CSS grown material is well suited for optoelectronic applications. In other words, presence of a single peak in the PL spectra can be attributed to absence of large concentrations of native defects that may form during a film growth process. This result is supported by the EDS, SEM and XRD measurements presented

above, which demonstrated good crystallinity and proper stoichiometry.

Figure 6a shows the typical intensity-dependent I–V characteristics of the fabricated devices for DC bias ranging from −4 to 4 V. Illuminated data at different wavelengths as well as data obtained in the dark are shown in this figure. As can be seen, the I–V curves at all wavelengths are near-symmetrical and they display an ohmic behavior. Significant changes in the electrical resistance value can be observed as the wavelength is varied from blue to red, the photo-current increasing with shorter wavelengths. At shorter wavelengths photocurrent becomes greater since the number of electron-hole pairs generated by the high-energy photons increases. This may be due to band-to-band transitions as well as some transitions involving defect levels within the bandgap. From the data obtained under blue light, the photo current/dark current ratio was calculated to be 751 at the bias of 2 V. This large number can be explained by the fact that CdSe film has low defect concentration, has a single phase and good surface morphology from the growth process. The resistivity and the carrier concentration at room temperature in the dark were found to be 4.2×10^4 Ω cm and 4.4×10^{12} cm^{-3}, respectively for these films.

Figure 6b shows the photocurrent-time switching properties of the photodetector at 10 V bias when

Fig. 6 The **a** current–voltage, **b** current–time, **c** photocurrent–power and **d** responsivity–wavelength curves of CdSe photodetector
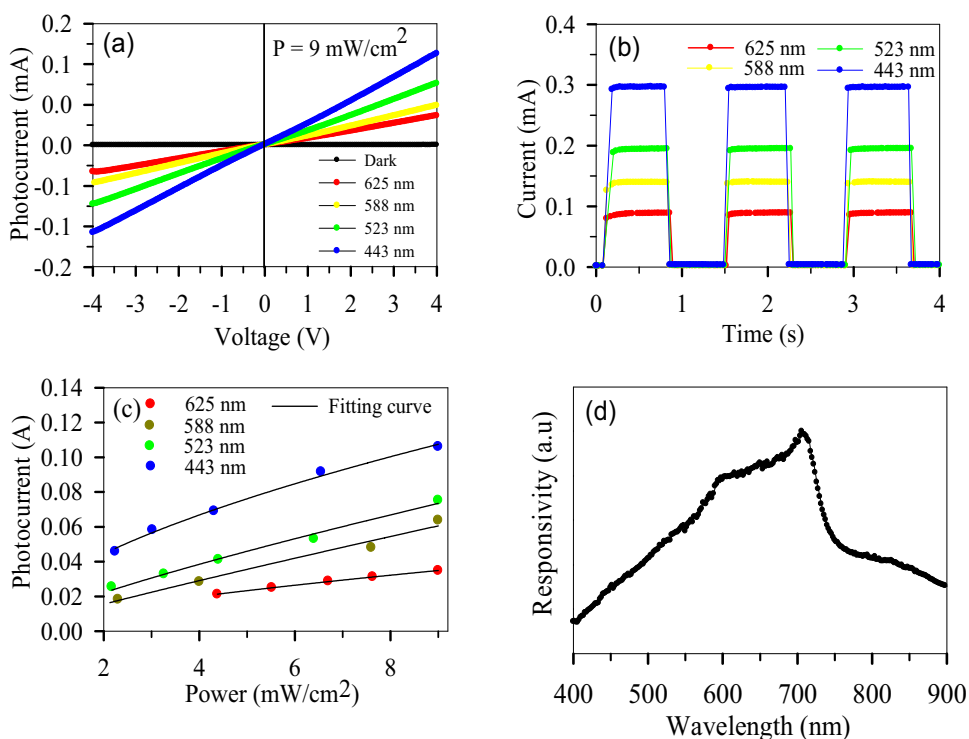
different wavelength light was switched on and off, sequentially. Results show rapid current rise and decay. It should be noted that the highest photocurrent value for the CdSe sample was obtained when illuminated with a wavelength of 443 nm. When rise and fall times were compared at different wavelengths (see Table 2), it was observed that the time difference between the rise and fall times (recovery time) changed as a function of wavelength. The shortest recovery time was 5ms at the wavelength of 588 nm.

Equation (2) below was used to obtain the photo-response of the device;

$$R = \frac{I_p}{AP_{in}},\tag{2}$$

where A is the area, I_P is the photocurrent and P_{in} is the intensity of the incident light. Detectivity ($D*$) can be calculated from Eq. 3. using the photo-response value;

$$D^* = R\sqrt{\frac{A}{2eI_d}},\tag{3}$$

where, e and I_d represent the electronic charge and the measured dark current, respectively [12].

Responsivity (R) and Detectivity (D) values calculated for the CdSe sample are given in Table 2. As can be seen from this table, the R and D values increase with decreasing value of the light wavelength.

Wavelength dependent behavior of photodetector parameters can be explained by presence of impurity levels that can act as traps or recombination centers for the excited charge carriers. The generated charge carriers with lower energy might primarily fill the impurity levels located between the valance band and the conduction band. This means that the photo-generated charge carriers with smaller energy may be captured with the defect/impurity levels placed in the band

structure. For this reason, they would have small contribution to photocurrent [22]. It should be noted that when R and D values of thin film and nanowire/nanoribbon-based photodetectors are compared, it is often found that these values are quite high in nanowire or ribbon materials. This situation is explained by presence of deep level states in the nanomaterials, which considerably extend the lifetime of photo-generated electrons by limiting electron-hole recombination [10]. It is also reported that high surface-to-volume ratio of nanomaterials increase their photocurrent carrying capacity [14].

The rise and fall times of the photodetector were calculated based on the photocurrent-time graph (see Fig. 6b) and are given in Table 2. The light intensity during these measurements was 9 mW/cm^2. As can be seen from this data, the calculated rise time values are higher than the fall time values at each wavelength. This is a previously observed and reported phenomenon [15]. Shelke et al. found that the fall time and the rise time of CdSe based devices fabricated by spray pyrolysis were 95 and 24 ms, respectively. They attributed this variation to the density of defects and traps that may be formed during the growth of the semiconductor compound [12].

The photocurrent-light intensity dependence measured at different wavelengths are given in Fig. 6c. This relationship can be represented by the equation; $I = AP^\theta$, where A is a constant, and the exponent θ determines the response of the photocurrent to light intensity. By fitting the experimental data to this relationship, the value of θ was estimated to be between 0.57 and 0.91 for different wavelengths. The highest value of θ was obtained in yellow light, while the lowest value was obtained under blue light. These results are consistent with those reported for CdSe nanowires and nanoribbons. The variation of θ values between 0.5 and 1 can be interpreted by a series of complex processes such as electron-hole generation, band-to-band recombination, recombination through defects in the bandgap, and trapping, while a value of $\theta < 0.5$ signifies influence of traps and recombination through defects [23]. The spectral responsivity of CdSe thin films at 10 V bias voltage under a light intensity of 9 mW/cm^2 is given in Fig. 6d. It is observed from this data that the spectral responsivity value increases linearly in the wavelength range of 400–600 nm. The rate of increase declines between 600–650 nm, and increases again in the 650–700 nm range. The maximum responsivity was observed at 714 nm. This is

Table 2 Photodetector parameters of CdSe thin films with respect to wavelength of electromagnetic illumination

Samples	λ (nm)	Rise time τ_{rise} (ms)	Fall time τ_{fall} (ms)	R (A/W)	$D*$ (Jones)
CdSe	625	37	25	1.83E–01	1.54E+09
	588	31	26	2.46E–01	2.07E+09
	523	68	33	3.84E–01	3.23E+09
	443	63	38	5.69E–01	4.79E+09

consistent with the band gap value calculated by the Tauc method and determined by the PL measurement.

Mechanism of photodetector performance can be described as follows: Photons are absorbed in the photodetector semiconductor material generating electron-hole pairs. These charge carriers are separated by the applied electric field and produce a current proportional to the incident photon flux. In electrical measurements carried out in air, oxygen molecules are adsorbed on the surface of CdSe semiconductor and capture free electrons on the photodetector surface. As a result, a depletion layer is formed, which leads to high resistivity under dark conditions. When different wavelengths of light irradiate the sample, they cause more electron hole pair generation. Free holes separated by the applied electric field are transported to the surface of the sample and contribute to the desorption of oxygen resulting in an increase in the photocurrent by decreasing the width of the depletion layer [24].

4 Conclusion

In this study, CdSe thin films were grown on glass substrates by Close Space Sublimation (CSS) method. The films were analyzed through several characterization techniques and they were used for photodetector fabrication. XRD data showed that CdSe layers grown by CSS had single-phase hexagonal structure with (002) preferred orientation. Any secondary phase formation and phase segregations were not observed. SEM surface and cross-sectional images revealed a microstructure comprising large and small faceted grains with size in the range of 0.5–1.0 μm. The band gap was determined to be 1.73 eV through transmission measurements. PL spectra showed a peak at 715 nm that corresponds to the band gap value obtained from the transmission measurement. This result can be explained by the fact that PL response was dominated by free carrier-to-band and/or band-to-band optical transitions. The photodetector performance was investigated at wavelengths of 443, 523, 588 and 625 nm. Photo-current was found to increase with decreasing wavelength. Overall, with this study, we have demonstrated that good quality CdSe thin films can be produced with the CSS method, which is a proven large-scale manufacturing technique. We also showed that CSS grown CdSe layers have a high potential to be used as photodetectors.

Author contributions

MAO: Conceptualization, Methodology, Writing—Original Draft, Validation, Investigation, Writing—review& editing. BMB: Writing—Original Draft, Validation, Investigation, Writing—review & editing. İP: Sample preparation, Investigation. MT: Sample preparation, Investigation. TK: Sample preparation, Investigation. EB: Conceptualization, Methodology, Writing—Original Draft, Validation, Investigation, Writing—review& editing.

Data availability

The data that support the findings of this study are available from the corresponding author upon reasonable request.

Declarations

Conflict of interest The author(s) declare that they have no competing financial interests or personal relationships that could have appeared to influence the work reported in this paper.

Ethical approval This article does not contain any studies involving animals performed by any of the authors. Also, this article does not contain any studies involving human participants performed by any of the authors.

References

1. O. Olusola, O. Echendu, I. Dharmadasa, Development of CdSe thin films for application in electronic devices. J. Mater. Sci. Mater. Electron. **26**, 1066–1076 (2015)
2. S. Kumari, G. Chasta, R. Sharma, N. Kumari, M. Dhaka, Phase transition correlated grain growth in CdSe thin films: annealing evolution to cadmium chloride activation. Phys. B Condens. Matter **649**, 414422 (2023)
3. A. Çiriş, B.M. Başol, Y. Atasoy, A. Karaca, M. Tomakin, T. Küçükömeroğlu, E. Bacaksız, Effect of ultra-thin $CdSe_xTe_{1-x}$

interface layer on parameters of CdTe solar cells. Sol. Energy **234**, 128–136 (2022)

4. A. Çiriş, B.M. Başol, Y. Atasoy, A. Karaca, M. Tomakin, T. Küçükömeroğlu, E. Bacaksız, Processing CdS-and CdSe-containing window layers for CdTe solar cells. J. Phys. D Appl. Phys. **54**, 215103 (2021)

5. S. Kumari, S. Chuhadiya, D. Suthar, M. Himanshu, N. Kannan, M.J. Kumari, J. Dhaka, Activation of thermally evaporated CdSe films employing different halides: an evolution to ion size impact on grain growth. J. Mater. Sci. **57**, 19466–19489 (2022)

6. S. Kumari, G. Chasta, Himanshu, N. Kumari, M. Dhaka, Annealing evolution to MgCl₂ treated CdSe absorber layers for solar cells. J. Mater. Sci. Mater. Electron. **34**, 1420 (2023)

7. A. Çiriş, B.M. Başol, Y. Atasoy, A. Karaca, T. Küçükömeroğlu, M. Tomakin, J. Bacaksiz, Deposition of CdSeTe alloys using CdTe—CdSe mixed powder source material in a close-space sublimation process. J. Mater. Sci. Mater. Electron. **32**, 9685–9693 (2021)

8. C. Li, F. Wang, Y. Chen, L. Wu, J. Zhang, W. Li, X. He, B. Li, L. Feng, Characterization of sputtered CdSe thin films as the window layer for CdTe solar cells. Mater. Sci. Semicond. Process. **83**, 89–95 (2018)

9. K.Y. Zhang, C.G. Hu, Y.S. Tian, C.H. Zheng, B.Y. Wan, Stable and highly photosensitive device of CdSe nanorods. Phys. E-Low Dimensional Syst. Nanostruct. **43**, 943–947 (2011)

10. Z. Hu, X. Zhang, C. Xie, C. Wu, X. Zhang, L. Bian, Y. Wu, L. Wang, Y. Zhang, J. Jie, Doping dependent crystal structures and optoelectronic properties of n-type CdSe:Ga nanowries. Nanoscale. **3**, 4798–4803 (2011)

11. D. Alagarasan, S. Varadharajaperumal, K.D.A. Kumar, R. Naik, A. Arunkumar, R. Ganesan, G. Hegde, E.E. Massoud, Optimization of different temperature annealed nanostructured CdSe thin film for photodetector applications. Opt. Mater. **122**, 111706 (2021)

12. N.T. Shelke, S.C. Karle, B.R. Karche, Photoresponse properties of CdSe thin film photodetector. J. Mater. Sci. Mater. Electron. **31**, 15061–15069 (2020)

13. S.S. Kumar, S. Valanarasu, K.V. Gunavathy, S. Vinoth, K. Haunsbhavi, D. Alagarasan, K.D.A. Kumar, M. Ubaidullah, S.F. Shaikh, B. Pandit, Enhancing the photodetection property of CdSe thin films via thermal evaporation technique: role of substrate temperature. Phys. Scr. **97**, 055807 (2022)

14. H. Xu, L. Hao, H. Liu, S. Dong, Y. Wu, Y. Liu, B. Cao, Z. Wang, C. Ling, Flexible SnSe photodetectors with ultrabroad spectral response up to 10.6 μm enabled by photobolometric effect. ACS Appl. Mater. Interfaces **12**, 35250–35258 (2020)

15. M. Kumar, S. Rani, P. Vashistha, A. Pandey, G. Gupta, S. Husale, V. Singh, Low bias operated, fast response SnSe thin film Vis-NIR photodetector on glass substrate using one-step thermal evaporation technique. J. Alloys Compd. **879**, 160370 (2021)

16. L. Hao, Z. Wang, H. Xu, K. Yan, S. Dong, H. Liu, Y. Du, Y. Wu, Y. Liu, M. Dong, 2D SnSe/Si heterojunction for self-driven broadband photodetectors. 2D Mater. **6**, 034004 (2019)

17. H.S. Jagani, A. Patel, C. Vyas, J. Gohil, V. Pathak, Self-biased and biased photo-sensitivity of tin mono-selenide (SnSe) photonic crystal photodetector under poly/monochromatic light. Opt. Mater. **141**, 113898 (2023)

18. H. Yao, S. Luo, G.S. Duesberg, X. Qi, D. Lu, C. Yue, J. Zhong, Enhanced photoresponse of graphene oxide functionalised SnSe films. AIP Adv. (2018). https://doi.org/10.1063/1.5031066

19. J. Luschitz, B. Siepchen, J. Schaffner, K. Lakus-Wollny, G. Haindl, A. Klein, W. Jaegermann, CdTe thin film solar cells: interrelation of nucleation, structure, and performance. Thin Solid Films. **517**, 2125–2131 (2009)

20. R. Parsons, W. Wardzynski, A. Yoffe, The optical properties of single crystals of cadmium selenide. Proc. Royal Soc. Lond. Ser A Math. Phys. Sci. **262**(1961), 120–131 (1961)

21. Y.P. Gnatenko, P. Bukivskij, I.O. Faryna, A. Opanasyuk, M.M. Ivashchenko, Photoluminescence of high optical quality CdSe thin films deposited by close-spaced vacuum sublimation. J. Lumin. **146**, 174–177 (2014)

22. M. Zhong, X. Wang, S. Liu, B. Li, L. Huang, Y. Cui, J. Li, Z. Wei, High-performance photodetectors based on sb(2)S(3) nanowires: wavelength dependence and wide temperature range utilization. Nanoscale. **9**, 12364–12371 (2017)

23. V.T. Patil, Y.R. Toda, V.P. Joshi, D.A. Tayade, J.V. Dhanvij, D.N. Gujarathi, Surface morphological and optical properties of CdSe thin films by closed space sublimation technique. Chalcogenide Lett. **10**, 239–247 (2013)

24. S. Saeed, R. Dai, R.A. Janjua, D. Huang, H. Wang, Z. Wang, Z. Ding, Z. Zhang, Fast-response metal-semiconductor-metal junction ultraviolet photodetector based on ZnS:Mn nanorod networks via a cost-effective method. ACS Omega **6**, 32930–32937 (2021)